SMART CEMENT SYSTEM FOR REAL-TIME MONITORING OF FIELD WELL INSTALLATION AND VERIFICATION OF CEMENTED WELL PIEZORESISTIVE BEHAVIOR PHYSICAL MODEL TESTS

C. Vipulanandan Ph.D., P.E.

Center for Innovative Grouting Material and Technology (CIGMAT)
Department of Civil and Environmental Engineering
University of Houston, Houston, Texas 77204-4003

Abstract

In order to demonstrate the potential of the smart cement system (combination of smart cement and monitoring instrumentation) a steel casing was installed in the field and cemented using the piezoresistive smart cement. The field well with the smart cementing system was designed, built, and used to verify the concept of real time monitoring of the flow of drilling mud and smart cement and hardening of the cement in place. The well with 95/8 in diameter and 40 feet in length casing was installed in soft swelling clay soils to investigate the sensitivity of the smart oil well cement. A new method has been developed to measure the electrical resistivity of the materials using the two probe method. Using the new concept, it has been proven that the resistivity dominated the behavior of drilling fluid and smart cement. Alternative current with two probes was used to measure the changes in electrical properties of the smart cement. The well instrumentation was outside the casing with over 110 probes, 18 strain gages and 9 thermocouples. The multiple instrumentations were used to compare the sensitivity of each type of measurement such as resistivity, strain and temperature and various depths in the cement sheath. Change in the resistance of hardening cement was continuously monitored since the installation of the field well. Also material and system models developed during the different PHASES of this study are being verified in the field. In addition, the pressure testing showed the piezoresistive response of the hardened smart cement and a piezoresistive model has been developed to predict the pressure in the casing from the change in resistivity in the smart cement.

Introduction

Environmental and economic concerns with some of the reported cementing failures in the oil and gas industry have demanded for the development of new innovative technologies for real-time monitoring of the wells. Oil well cement serves many purposes in the cemented oil and gas wells. Foremost important among these is to form a sealing layer between the well casing and the geological formation referred to as the zone of isolation. Past four decades of offshore well failures in the offshore of U.S. have clearly identified cementing failures as the major cause for blowouts (Izon et al. 2007). Also the deep-water horizon blowout in 2010 in the Gulf of Mexico was due to cementing issues

(Carter et al. 2014; Kyle et al. 2014). Therefore, real-time monitoring and tracking the process of well cementing and the performance during the entire service life has become important to ensure cement integrity (Vipulanandan et al. 2014 (a)-(d); Zhang et al. 2010 (a)-(b)).

Smart Oil Well Cement

Cements such as Class G and Class H are considered to be two of the most used cements in OWC applications. These cements are produced by pulverizing clinker consisting essentially of calcium silicates (CanSimOp), with an addition of calcium sulphate ($CaSO4$) (John, 1992). Class H cement is produced by a similar process, except that the clinker and gypsum are ground relatively coarser than for a Class G cement, to provide a cement with a surface area generally in the range 220 - 300 m2/kg (John, 1992).

A smart cement has been developed (Vipulanandan et al. 2014a,b; Vipulanandan and Mohammed 2015a,b) which can sense any changes going on inside the borehole during cementing and during curing after the cementing job. The smart cement can sense the changes in the water cement ratio, different additives, and any pressure applied to the cement sheath in terms of piezoresistivity (Vipulanandan and Mohammed 2015a). The failure compressive strain for the smart cement was 0.2% at peak compressive stress (Vipulanandan et al. 2015b) and the resistivity change is of the order of several hundred making it over 500 times more sensitive.

Objective

The overall objective of this work was to demonstrate the monitoring of the installation of a field well and to verify the sensitivity of the piezoresistive smart cement to the changing surrounding conditions and the external stresses applied on it.

The specific objectives were as follows:

(1) Verify the smart cement system in the field by monitoring the changes in the electrical resistance during the installation and after cementing of the well.

(2) Compare the measured and predicted changes in the electrical resistance of the hardening smart cement sheath outside the casing.

(3) Verify the sensitivity of the piezoresistive smart cement response of the hardened smart cement sheath with applied pressures.

Theory and Concept

Impedance Model (Vipulanandan et al., 2013)

Equivalent Circuit.

It is important to identify the most appropriate equivalent circuit to represent the electrical properties of a material to characterize its performace with time. In this study, different possible equivalent circuits were analyzed to find an appropriate equivalent circuit to represent smart cement and drilling fluid.

Case 1: General Bulk Material –Capacitance and Resistance

In the equivalent circuit for Case1, the contacts were connected in series, and both the contacts and the bulk material were represented using a capacitor and a resistor connected in parallel (Fig. 1).

In the equivalent circuit for Case 1, Rb and Cb are resistance and capacitance of the bulk material, respectively; and Rc and Cc are resistance and capacitance of the contacts, respectively. Both contacts are represented with the same resistance (Rc) and capacitance (Cc), as they are identical. Total impedance of the equivalent circuit for Case 1 (Z1) can be represented as follows:

$$Z_1(\sigma) = \frac{R_b(\sigma)}{1+\omega^2 R_b^2 C_b^2} + \frac{2R_c(\sigma)}{1+\omega^2 R_c^2 C_c^2} - j\left\{\frac{2\omega R_c^2 C_c(\sigma)}{1+\omega^2 R_c^2 C_c^2} + \frac{\omega R_b^2 C_b(\sigma)}{1+\omega^2 R_b^2 C_b^2}\right\}, \qquad (1)$$

where ω is the angular frequency of the applied signal. When the frequency of the applied signal is very low, $\omega \to 0$, $Z_1 = R_b + 2R_c$, and when it is very high, $\omega \to \infty$, $Z_1 = 0$.

Case 2: Special Bulk Material - Resistance Only

Case 2 is a special case of Case 1 in which the capacitance of the bulk material (C_b) is assumed to be negligible (Fig. 2). The total impedance of the equivalent circuit for Case 2 (Z_2) is as follows:

$$Z_2(\sigma) = R_b(\sigma) + \frac{2R_c(\sigma)}{1+\omega^2 R_c^2 C_c^2} - j\frac{2\omega R_c^2 C_c(\sigma)}{1+\omega^2 R_c^2 C_c^2}. \qquad (2)$$

When the frequency of the applied signal is very low, $\omega \to 0$, $Z_2 = R_b + 2R_c$, and when it is very high, $\omega \to \infty$, $Z_2 = R_b$ (Fig. 3).

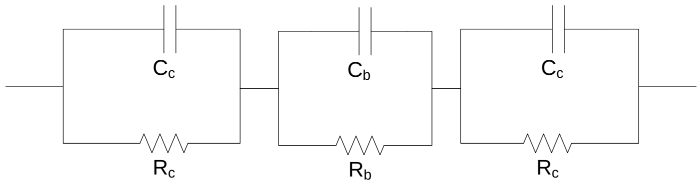

Figure 1. Equivalent Circuit for Case1

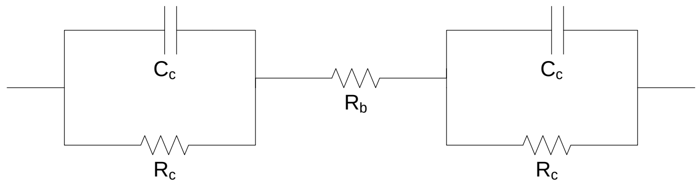

Figure 2. Equivalent Circuit for Case 2

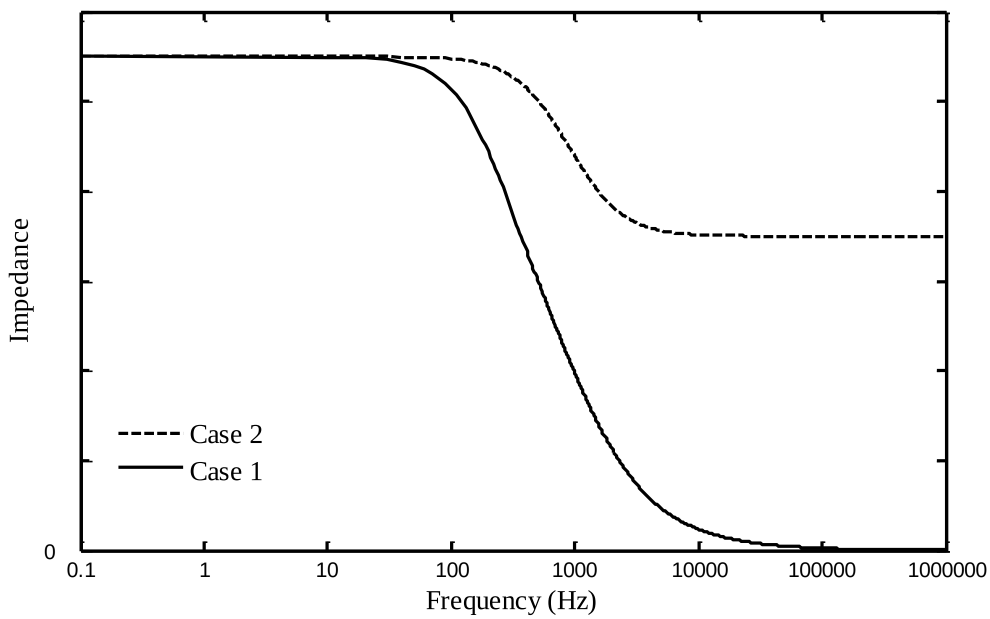

Figure 3. Comparison of Typical Responses of Equivalent Circuits for Case 1 and Case 2

The shape of the curves shown in Fig. 3 is very much influenced by the material response and the two probe instruments used for monitoring. Testing of smart cement and drilling fluid clearly indicated that Case 2 represented their behavior and hence the bulk material properties can be represented by resistivity and was characterized at a frequency of 300 kHz using the two probes in this study.

Resistance and Resistivity

After years of studies and based on the current study on well cements and drilling muds, electrical resistivity (ρ) was selected as the sensing property for both cements and drilling muds. This is unique since in that the same monitoring system can be used to evaluate the performance of cement and drilling muds. Hence, two parameters (resistivity and change in resistivity) will be used to quantify the sensing properties as follows:

$$R = \rho\ (L/A) = \rho\ K \tag{3}$$

where:

R = electrical resistance
L = Linear distance between the electrical resistance measuring points
A = effective cross sectional area
K = Calibration parameter is determined based on the resistance measurement method

Normalized change in resistivity with the changing conditions can be represented as follows:

$$\Delta\rho/\rho = \Delta R/R \tag{4}$$

Resistivity of the materials (ρ) to the changes (composition, curing, stress, fluid loss, and temperature) has been quantified. Correlating the changes, such as composition, curing, stress, cracking, fluid loss, and temperature, to the resistivity (ρ) (Eqn. (3)) and change in resistivity ($\Delta\rho$) (Eqn. (4)) will support the monitoring of the materials (cement and drilling fluid) behavior.

Test Site

After reviewing a few potential test sites, Energy Research Park (ERP) at the University of Houston, Houston Texas was selected to intall the field well. Many factors including geology, swelling and soft clays, changing surrounding conditions (weather, active zone in the ground), environmental regulations and accessibility to the site for long-term monitoring had to be considered in selecting the test site since the focus of the study was to demonstrate the sensitivity of the smart cemented field well. The selected site had swelling clays with fluctuating moisture conditions (active zone) which represents the nearly the worst conditions that could be encountered when installing oil wells. The top 20 feet of the soil was swelling clay soil with liquid limit of over 50%. Based on ASTM classification, this soil was characterized as CH soil. The active zone in the Houston area is about 15 feet, indicating relatively large moisture fluctuation in the soil causing it to swell and shrink. The water table was 20 feet below the ground and soil below the water table was also clay with less potential for swelling and the liquid limit was below 40%. Based on ASTM classification, this soil was characterized as CL soil.

Instrumentation

It has been shown that the two probes with AC current can be used to determine the electrical resistance changes in the smart cement and drilling fluid (Vipulanandan 2015 (a)-(d)). It was also important use other standard tools for measuring the changes in the cement sheath and compares it to the resistance changes. Because of practical reasons no instrument was placed on the casing and totally an independent system was developed to be place in the cement sheath. As shown in Fig. 4 and Fig. 5 probes were placed at various vertical depths. In the vertical direction the probes were placed at 15 levels (Fig. 4). Also eight probes (A, B, C, D, E, F, G and H) were placed horizontally at each level. Also nine stain gages and nine thermocouples were included in the instrumentation (Fig. 4). When a vertical resistance measurement is referred as E 2-3, it refers to the measurement in column E between vertical levels 2 and 3. Similarly horizontal resistance measurement is referred as E2-F2, measurement was done at vertical level 2 between probe E and probe F horizontally.

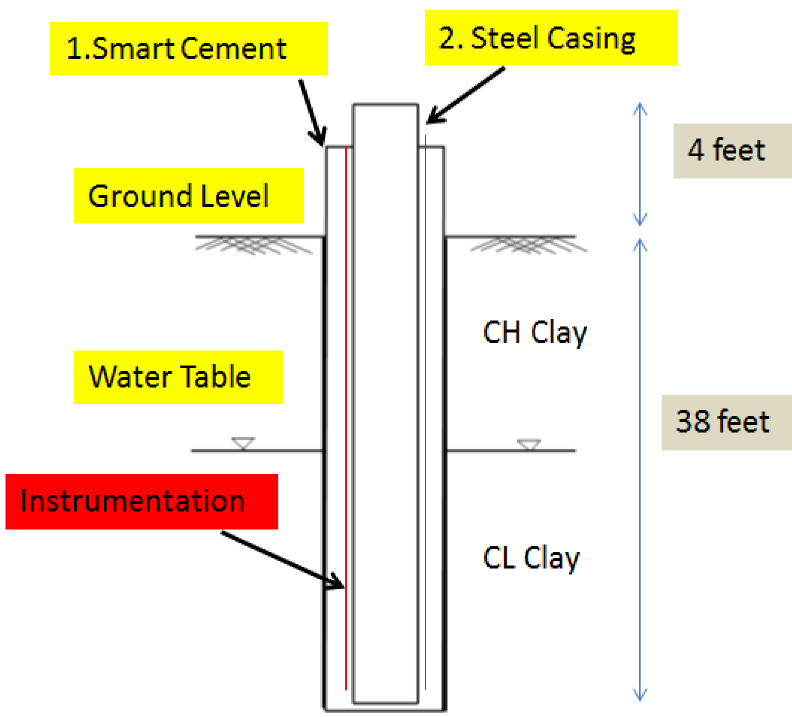

Figure 4. Schematic View of the Field Well with the Instrumentation

Installation of the Field Well

A commercial company familiar with the drilling and cementing wells in an urban setting was selected to install the field well. A very large drilling truck with drilling with 14 in diameter drill was used to drill the hole and place the 95/8 in diameter standard steel casing. The total length of the casing was 42 feet and needed pieces (including well head and needed connections to lift the casing) were welded together to make a single unit. Initial 15 feet was drilled without any drilling fluid. Polymer based drilling fluid was used to drill the rest of the borehole. After completing the drilling the casing and the instrumentation units were centered and lowered into the borehole. Initial resistivity of vertical probes were measured (Fig. 6) in the air which was about 1000 Ω. The casing and the instrumentations were lowered into the borehole and the cement was pumped from the bottom of the borehole and was driving the drilling mud up the borehole. Monitoring of the resistance between the probes, temperature and stains (strain gages) were measured.

Materials and Methods

In this study, polymer drilling fluid and smart cement were used.

Polymer drilling fluid

Polymer based drilling fluids are used to drill through reactive geological formation. Since this study the drilling was to be done through swelling soft montmorillonite clay, polymer drilling fluid was used. It is less reactive with the clay formations and also controls the fluid loss into the formations. The density of the polymer drilling fluid was 8.7 ppg and the electrical resistivity was in the range of 2 Ω.m to 3 Ω.m.

Smart cement

Cement slurry was prepared using a water-to-cement ratio of about 0.6, making the mixing and pumping easier in the field. . The cement was modified with an addition of 0.075 percent conductive filler by total weight of the cement slurry. The initial resistivity of the cement slurry was in the range of 1.20 to 1.24 Ω.m. Total of 42 samples were collected for characterizing the smart cement behavior.

Initial resistivity of smart cement slurry

Two Different methods were used for electrical resistivity measurements of oil well cement slurries. To assure the repeatability of the measurements, the initial resistivity was measured at least three times for each cement slurry and the average resistivity was reported. The electrical resistivity of the cement slurries were measured using:

Conductivity probe

Commercially available conductivity probe was used to measure the conductivity (inverse of resistivity) of the slurries. In the case of cement, this meter was used during the initial curing of the cement. The conductivity measuring range was from 0.1μS/cm to 1000 mS/cm, representing a resistivity of 0.1Ω.m to 10,000 Ω.m.

Digital resistivity meter

Digital resistivity meter (used in the oil industry) was used measure the resistivity of fluids, slurries and semi-solids directly. The resistivity range for this device was 0.01Ω-m to 400 Ω.m.

The conductivity probe and the digital electrical resistivity device were calibrated using standard solution of sodium chloride (NaCl).

Resistivity of smart cement

In this study high frequency AC measurement was adopted to overcome the interfacial problems and minimize the contact resistances. Electrical resistance (R) was measured using LCR meter during the curing time. This device has a least count of 1 μΩ for electrical resistance and measures the impendence (resistance, capacitance and inductance) in the frequency range of 20 Hz to 300 kHz. Based on the impedance (z) – frequency (f) response it was determined that the smart cement was a resistive material (Vipulanandan et al. 2013). Hence the resistance measured at 300 kHz using the two probe method was correlated to the resistivity (measured using the digital resistivity device) to determine the K factor (Eqn.1) for a time period of initial five hours of curing. This K factor was used to determine the resistivity of the cement with the curing time. The typical trend between impedance and frequency observed during the curing of smart cement is shown in Fig. 2.

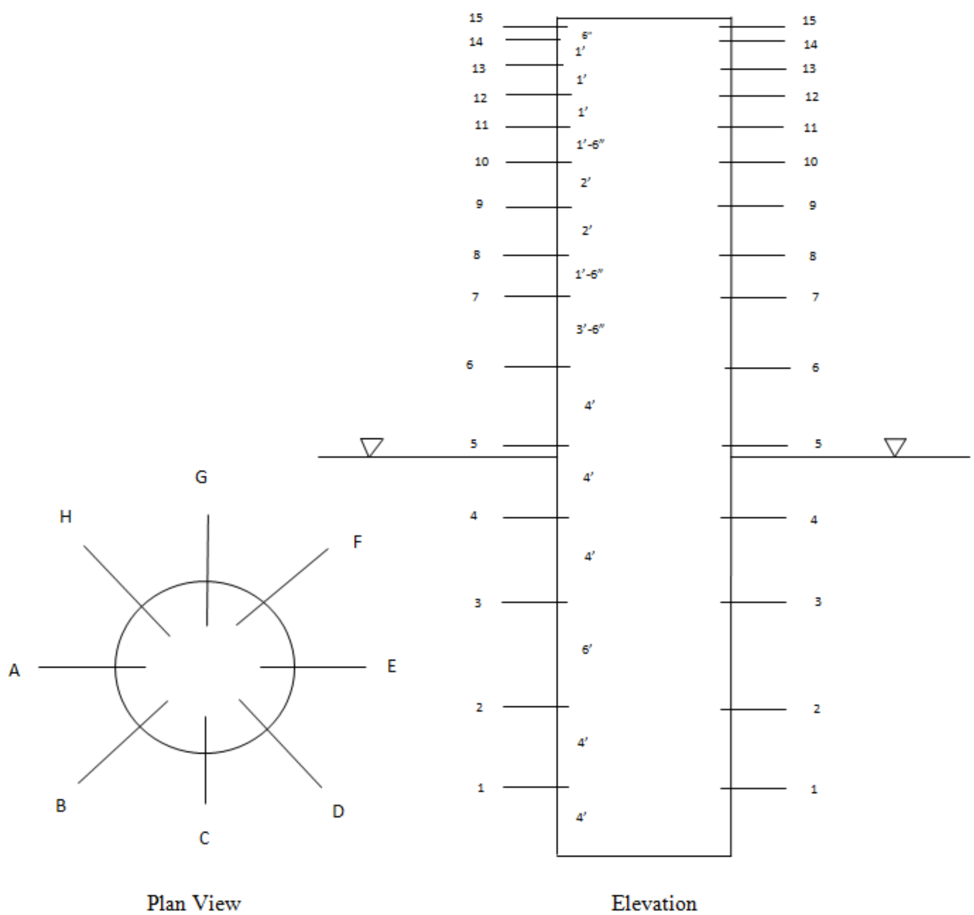

Figure 5. Vertical (Elevation) and Horizontal (Plan) Layout of the Probes in the Smart Cemented Well

Piezoresistivity test

Piezoresistivity describes the change in electrical resistivity of a material under stress. Since oil well cement serves as pressure-bearing part of the oil and gas wells in real applications, the piezoresistivity of smart cement (stress – resistivity relationship) with different w/c ratios were investigated under compressive loading at different curing times. During the compression test, electrical resistance was measured in the direction of the applied stress. To eliminate the polarization effect, AC resistance measurements were made using a LCR meter at frequency of 300 kHz (Vipulanandan et al. 2013).

Results and Discussion

Installation

During initial 20 feet of drilling no drilling fluid was used. In order to stabilize the borehole polymer drilling fluid was used drill the rest of the hole. The total length of the borehole was about 38 feet. The steel casing with external instrumentation was lowered into the borehole and the changes in the resistance was started to be monitored. The vertical resistance between the adjacent probes were of the order of 1000 Ω as shown in Fig. 6. The resistance between probes A1-A2 represented in the Fig. 6 by symbol a reduced to about 200 Ω when probe 2 reached the drilling fluid. Similarly the resistance between other adjacent probes reduced when the probes were submerged into the drilling fluid. In 20 minutes the probe A10-A11 (symbol j) reduced to 200 Ω indicating the rate of lowering of the casing about 38 feet, This sudden changes in the resistance clearly showed the level of the casing that was lowered and submerged in the drilling fluid.

The cementing was started after 30 minutes. The resistance of probe A1-A2 (symbol a) reduced to about 20 Ω after 35 minutes indicating that cement has reached vertical level 2. Rising of the cement lowered the resistances as shown in the Fig. 7. In about 80 minutes the cement reached the vertical level of 11 and the resistance dropped 20 Ω (A10-A11) (symbol j). The electrical resistance changes observed during the placement of the drilling fluid and cement was very similar to the laboratory model test (Vipulanandan et al. 2015 (c)). Cement was displacing the drilling fluid at the top of the borehole and the vertical resistance (A12- A13) (symbol l) dropped from 1000Ω to 200Ω indicating that drilling fluid has reached level 13 after 40 minutes of the operation.

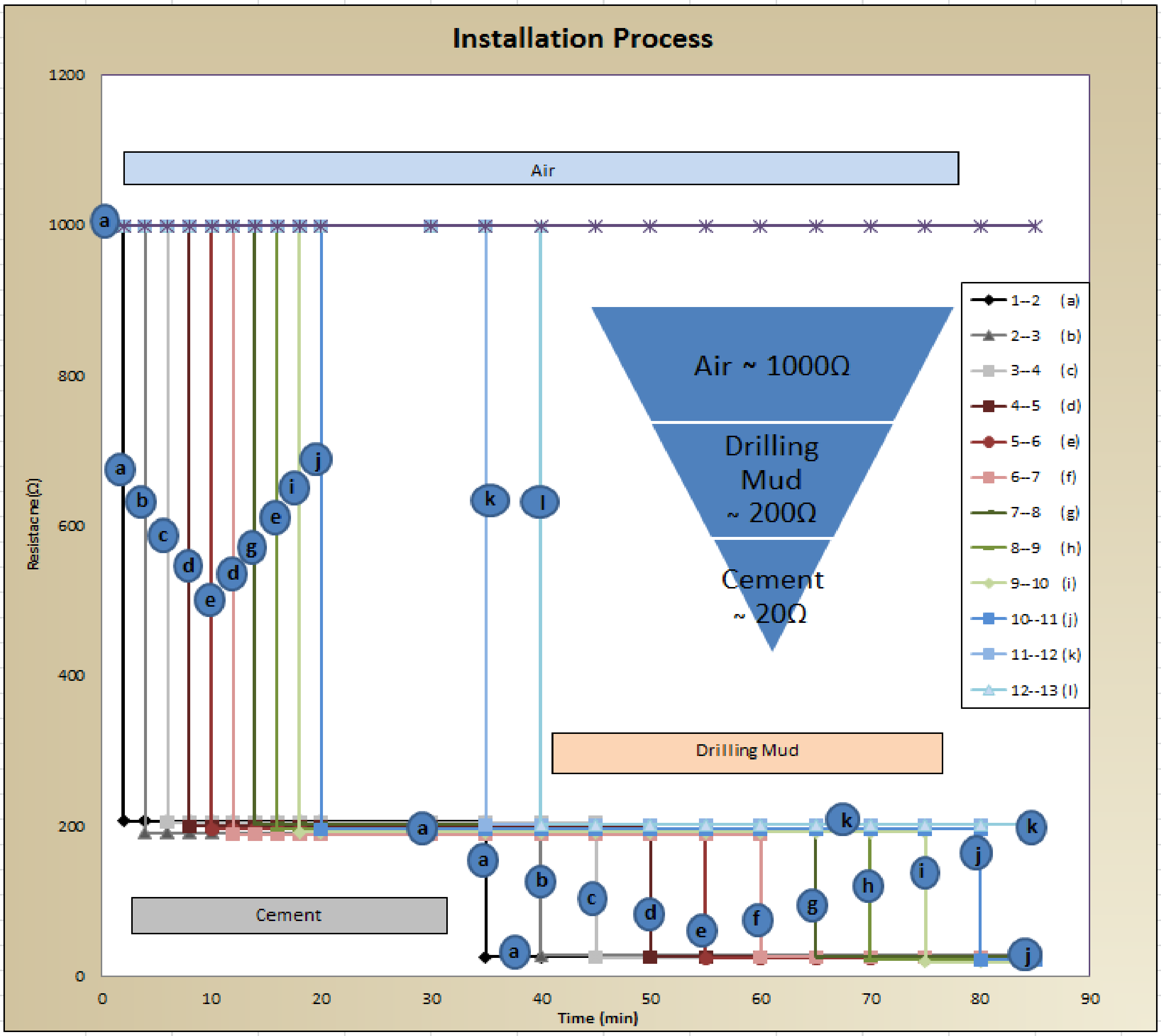

Figure 6. Vertical Resistance Changes for Drilling Fluid and Cement Slurry Reaching Various Levels

Cement Curing

First Day

Typical changes measured in the strain gage, thermocouple and resistance probe during the first day of curing of the cement in the borehole are shown in Fig. 7. The thermocouple shows the increase in the temperature due to the hydration of the cement. The cement initial resistance was 24 Ω and reduced to about 20 Ω and then increased to about 50 Ω in 24 hours, a 150% change. The change in the strain gage resistance of 120 Ω was very small. Hence change in the electrical resistance was the largest of the parameter that are being monitored during the hydration of the cement.

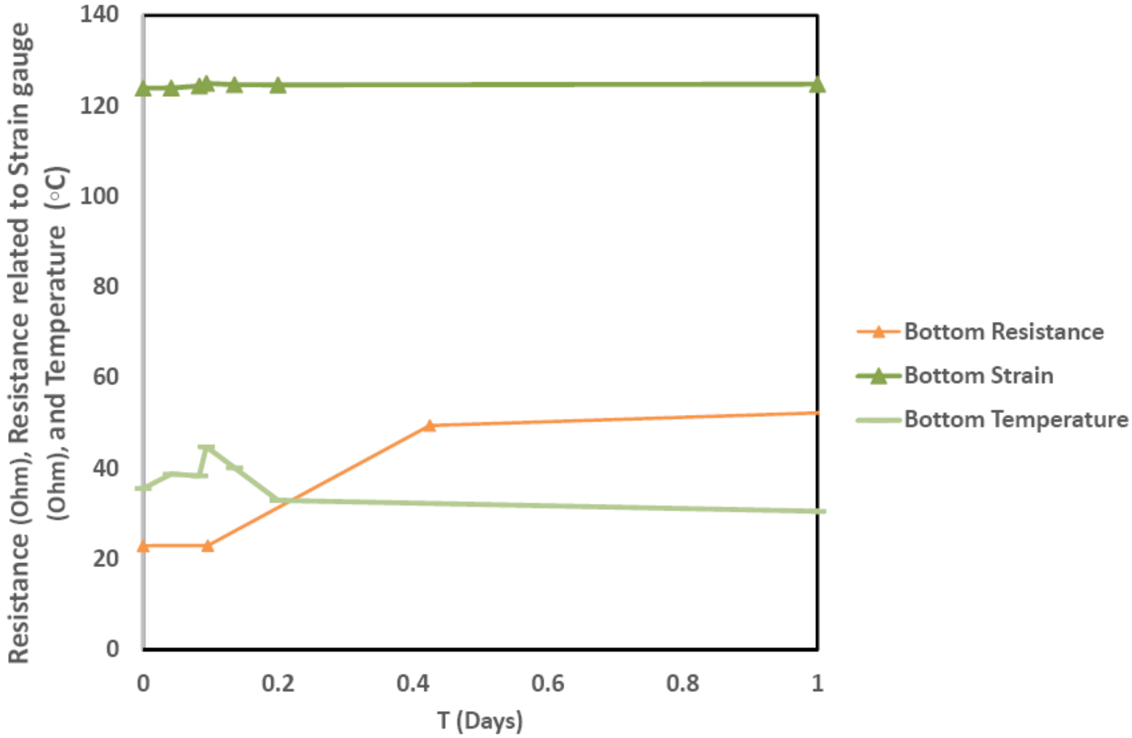

Figure 7. Variation in the Strain Gage, Temperature and Smart Cement Resistance during the First Day of Cement Curing in the Borehole.

Piezoresistive Relationship

Collected cement samples were cured under different conditions and the tested compressive loading after 45 days to determine the piezoresistivity. The bottom and middle level samples were cured under water and the top level sample was cured under room condition (23oC and relative humidity of 50%). For samples cured under water the change in the resistivity at peak stress varied from 70% to 160% based on the different batches of mixing of the smart cement (Fig. 8). The failure compressive strain for the smart cement was 0.2% at peak compressive stress (Vipulanandan et al. 2015b) and hence the resistivity change was 350 to 800 times more sensitive.

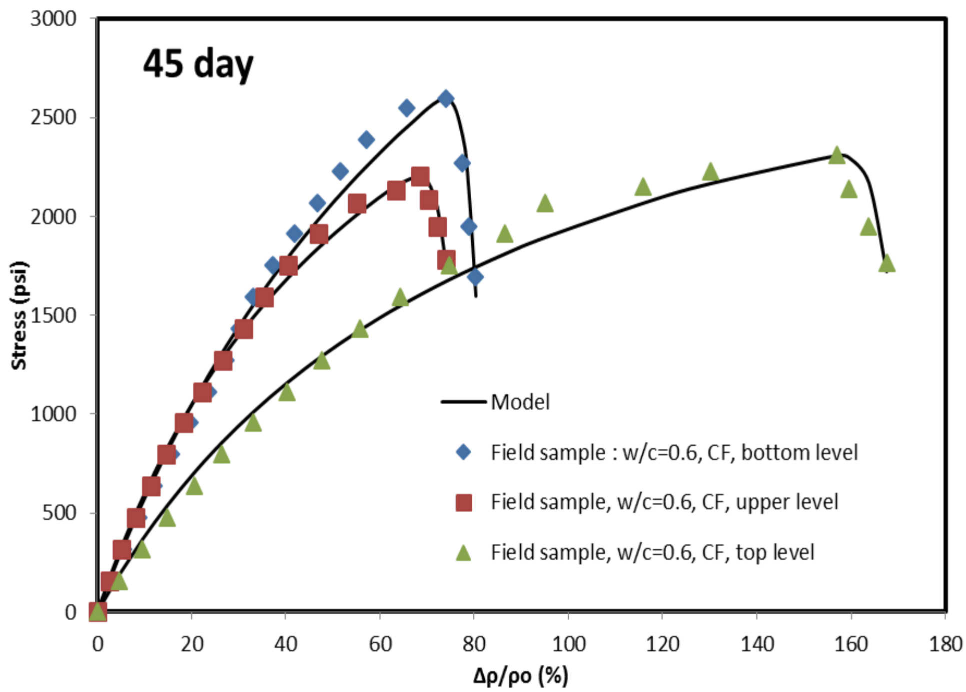

Figure 8 Piezoresistive Behavior of the Smart Cement at Various Depths in the Field Well

Based on experimental results, p-q model was modified to predict the change in electrical resistivity of cement during with applied compressive stress for 45 days of curing. The model is defined as follows:

$$\frac{\sigma}{\sigma_f} = \left[\frac{\frac{x}{x_f}}{q_2 + (1 - p_2 - q_2)\frac{x}{x_f} + p_2 \left(\frac{x}{x_f}\right)^{\left(\frac{p_2 + q_2}{p_2}\right)}} \right] \tag{5}$$

where σ is the stress (MPa); σ_f: compressive stress at failure (MPa); $x = \left(\frac{\Delta\rho}{\rho_o}\right) * 100$: Percentage of change in electrical resistivity due to the stress; $x_f = \left(\frac{\Delta\rho}{\rho_o}\right)_f * 100$: Percentage of change in electrical resistivity at failure; Δρ: change in electrical resistivity; ρ_o : Initial electrical resistivity (σ=0 MPa). The model parameter q_2 and p_2 are summarized in Table 1. The coefficient of determinations (R^2) varied from 0.98 to 0.99.

Table 1. Piezoresisitive Model Parameters

Borhole Level	p_2	q_2
Bottom level	0.011	0.55
Upper level	0.012	0.46
Top level	0.005	0.34

Resistivity of the curing cement sheath with time

The resistivity of the cement slurry with curing time of up to 110 days was determined from the field samples in small molds (2 inches diameter and 4 inches height cylindrical mold) cured under different curing conditions. All field samples were first cured under room condition for one day then cured under no moisture loss condition (close to ground condition above the ground water), room condition and under water (representing the condition underwater. Samples cured under room condition had a weight loss of 2.8% after 110 days. The electrical resistivity was determined for a sample cured under moisture control (no moisture loss) condition, for a sample cured under room condition (a moisture loss of 2.8 % was calculated up to 110 days), and for a sample cured under water condition (a moisture gain of 1.2 % after 110 days) .

At least three specimens were tested under each condition and the average results are discussed. The change of electrical resistivity with curing time for the cement specimens cured under different environments is shown in Fig. 9. The normal trend of the resistivity of the cured cement is that the resistivity decreased up to a certain time (tmin) and reached to a minimum resistivity (ρmin) and then starts increase with time. Hence the nonlinear model proposed by Vipulanandan and Paul (1990) was modified and used to predict the changes in the electrical resistivity of cement during hydration under different curing conditions and curing time. The proposed curing model is as follows:

$$\frac{1}{\rho} = \left(\frac{1}{\rho_{min}}\right)\left[\frac{\left(\frac{t+t_o}{t_{min}+t_o}\right)}{q_1+(1-p_1-q_1)*\left(\frac{t+t_o}{t_{min}+t_o}\right)+p_1*\left(\frac{t+t_o}{t_{min}+t_o}\right)^{\frac{q_1+p_1}{p1}}}\right] \quad (6)$$

Where, ρ is the electrical resistivity (Ω-m); ρ_{min} is the minimum electrical resistivity (Ω-m); t_{min} is the time to reach the minimum electrical resistivity (ρ_{min}). The model parameters were t_o, p_1 (t) and q_1 (t) and t was the curing time (min). The parameter q_1 represents the initial rate of change in the resistivity.

There are three characteristic resistivity parameters that can be used in monitoring the curing (hardening process) of the cement. The resistivity parameters are the initial resistivity (ρ_o), minimum electrical resistivity (ρ_{min}) and time to reach the minimum resistivity (t_{min}).

The resistivity shows an increasing trend with curing time (Fig. 9) which has been modeled with the curing model which is developed by modifying the p-q model proposed by Vipulanandan and Paul (1990) (Eqn. 6). The model parameters were for moisture control curing (zero weight loss): p_1=7.6, q_1=0.6, and t_o=70 min; for room curing: p_1=6.5, q_1=0.82, and t_o=72 min; and for under water curing: p_1=0.83, q_1=0.21, and t_o=58 min. (Table 2).

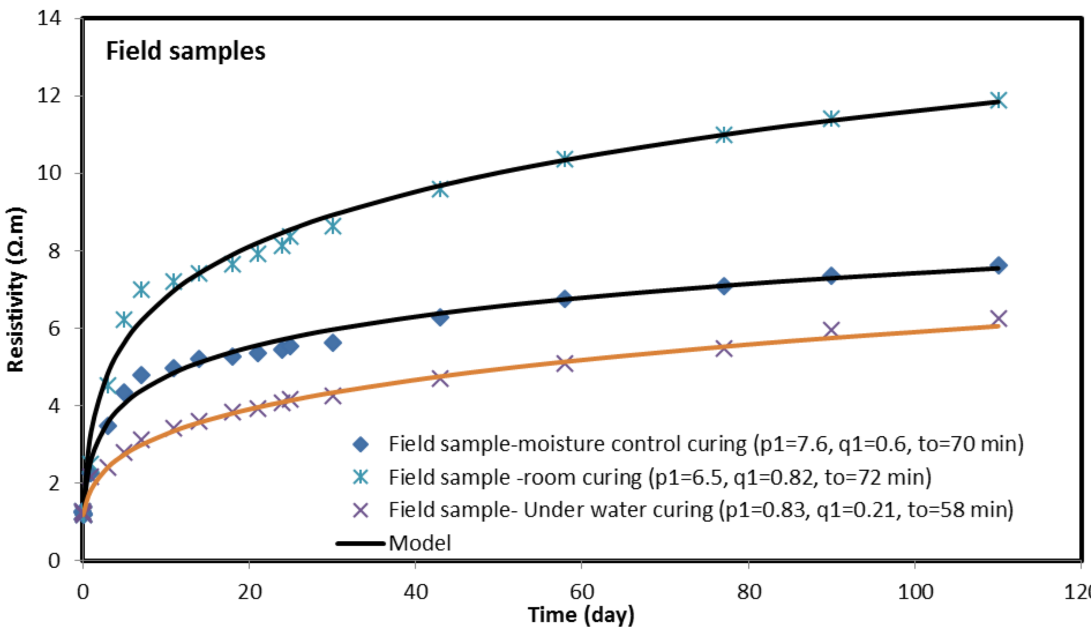

Figure 9 Variation of Smart Cement Resistivity with Curing Time for Samples Cured Under Room Condition (23°C and 50% Relative Humidity (RH)), Under Water and Zero Weight Loss.

The coefficient of determination (R^2) varied from 0.96 to 0.99 and the root mean square of error (RMSE) varied from 0.03 Ω.m to 0.72 Ω.m.

Table 2. Curing Model Parameters for Field samples

Curing Condition	Model Parameters				
	ρ_{min} (Ω.m)	t_{min} (min)	q_1	P_1	t_o (min)
Room curing	1.18	180	0.82	6.48	72
Moisture control curing	1.18	180	0.61	7.6	70
Under water curing	1.18	180	0.21	0.84	58

Prediction and Measured Resistance

The resistance measured on site can be predicted using Eqn. 3. Hence parameter K must be determined by calibrating the instrumentation.

Parameter K

The K parameter (i.e. L/A) for the wire setup A, B, C, D, E, F, G and H with the probe spacing were determined using the cement slurry. The resistivity of the cement slurry was measured by direct resistivity measurement device and the resistance between the two probes was measured using the LCR meter. The results of the K values are shown in Fig. 10 and the average value, maximum value, and minimum values are summarized in Table 3 for different wire combination.

For different wire combination, the average K parameter are found to be varied from 14.6

to 29.8 m-1 with standard deviations varying from 1.6 to 3.3 m-1 (Fig. 10 and Table 3).

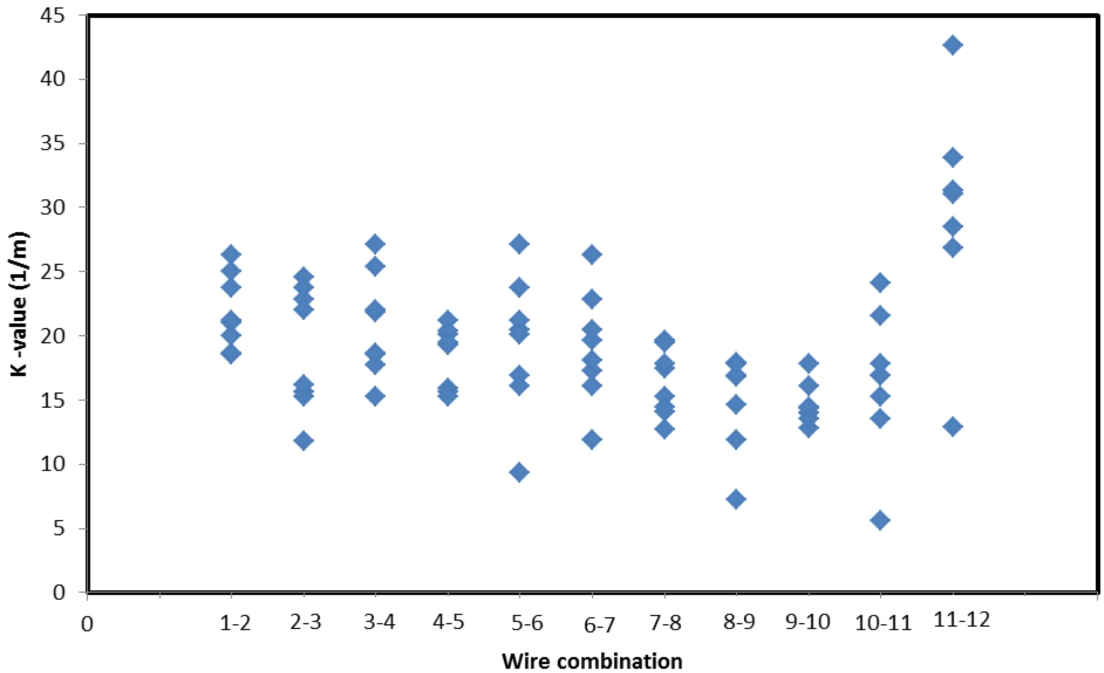

Figure10 Parameter K for Different Wire Combination for Instrumented Field Well

Table 3. Variations of parameter K for Different Probe Combination for the Field Well

Probes	1-2	2-3	3-4	4-5	5-6	6-7	7-8	8-9	9-10	10-11	11-12
Spacing	48 inches	72 inches	48 inches	48 inches	48 inches	42 inches	18 inches	24 inches	24 inches	18 inches	12 inches
Avg	21.8	19.0	20.8	18.4	19.4	19.1	16.4	15.1	14.6	16.5	29.8
Min	18.6	11.8	15.3	15.3	9.3	11.9	12.7	7.3	12.8	5.6	12.9
Max	26.3	24.6	27.1	21.2	27.1	26.3	19.7	17.9	17.8	24.1	42.6
Std. dev	1.9	1.8	2.0	1.4	2.4	2.4	2.6	2.8	1.6	2.5	3.3
No of data	16	16	16	16	16	16	16	16	16	16	16

Predicted (Electrical Resistance Model –ERM)

Vertical Resistance

Probe E2-E3: The measured vertical resistance between probes E2 and E3 (72 inches spacing) below the ground water are compared to the predicted resistance in Fig 11. The measured resistances during the period of 3 to 5 days were slightly higher than the predicted values. This may be because of the difference in the curing condition of the cement in the ground compared to the laboratory or small amount of clay soil contaminating the cement. . With increased curing the measured resistance values were within the predicted region. During the period of 110 days the electrical resistance changed from 24 Ω to 110 Ω, over 350% increase in the resistance.

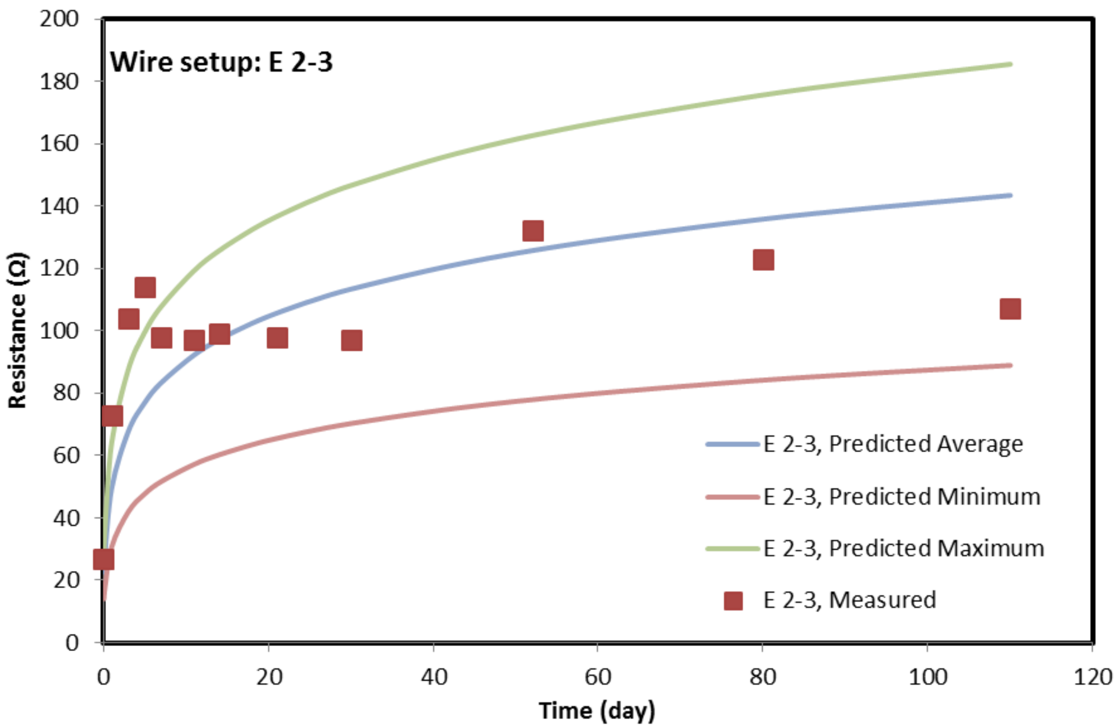

Figure 11. Comparing the Predicted and Measured Resistance for Vertical Probes E2-E3.

Probe E5-E6. The measured vertical resistance between probes E 5 and E6 (48 inches spacing) above the ground water are compared to the predicted resistance in Fig 12. The changes in the resistance are very similar to that was observed for probes E2-E3. The measured resistances during the period of 3 to 5 days were little higher than the predicted values. This may be because of the difference in the curing condition of the cement in the ground compared to the laboratory or small amount of clay soil contaminating the cement. . With increased curing the measured resistance values were within the predicted region. During the period of 110 days the electrical resistance changed from 20 Ω to 140 Ω, over 600% increase in the resistance.

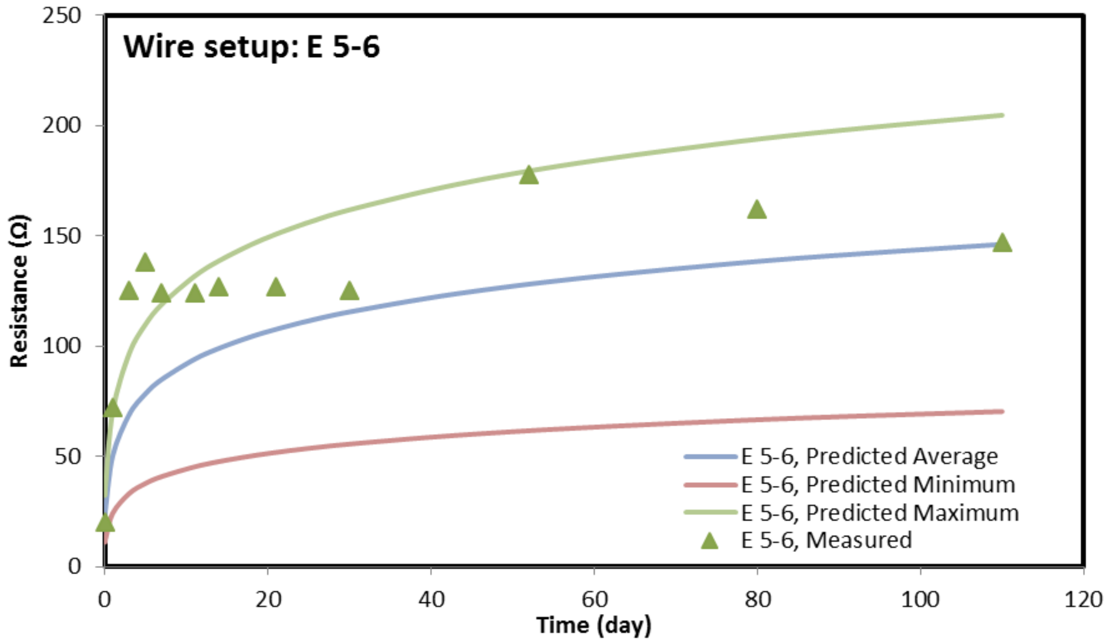

Figure 12. Comparing the Predicted and Measured Resistance for Vertical Probes E5-E6.

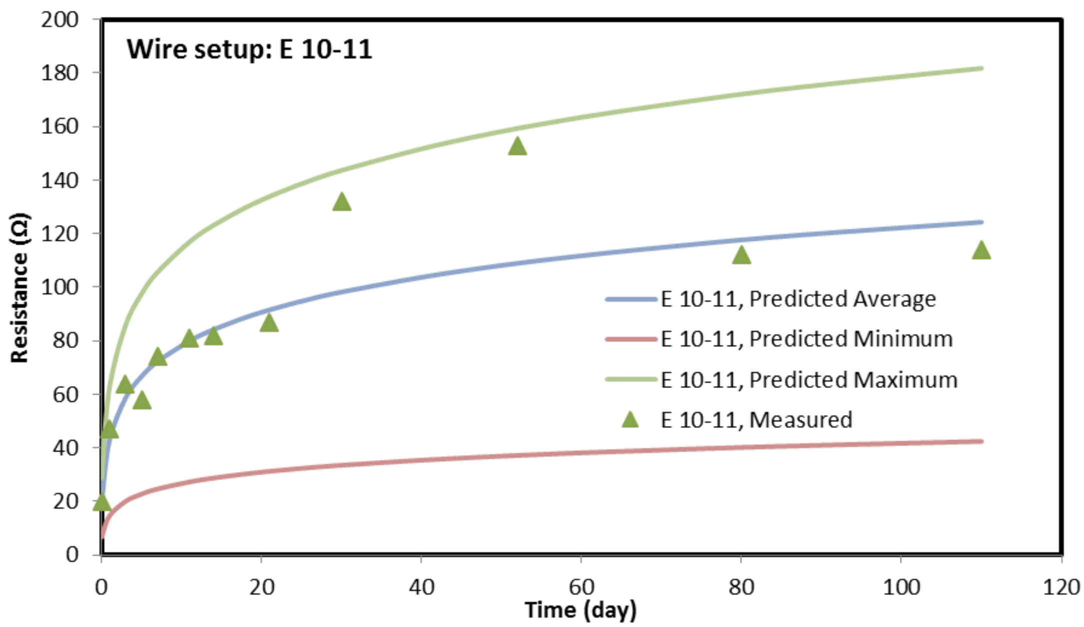

Figure 13. Comparing the Predicted and Measured Resistance for Vertical Probes E10-E11.

Probe E10-E11: The measured vertical resistance between probes E10 and E11 (18 inches spacing) close to the ground surface are compared to the predicted resistance in Fig 13. The changes in the resistance are very similar to that was observed for probes E2-E3 and E5-E6. With increased curing all the measured resistance values were within the predicted region. In this case all the measured resistances were within the predicted range. The measured resistances during the period of 35 to 55 days were little higher than the other resistance could be inditactive of the effect of the higher environmental temperature (hot weather during June-July in Houston) since E10-E11 is close to the ground surface. During the period of 110 days the electrical resistance changed from 18 Ω to 110 Ω, over 500% increase in the resistance.

Horizontal Resistance

Probe E10-F10: The measured horizontal resistance between probes E10 and F10 (5 inches spacing) close to the ground surface are compared to the predicted resistance in Fig 14. The changes in the resistance are very similar to that was observed for probes E2-E3 and E5-E6. With increased curing all the measured resistance values were within the predicted region. Unlike vertical Probe E10-E11, the measured resistances between probes E10 and F10 continuously increased and was not affected by the higher environmental temperature (hot weather during June-July in Houston) because the probes 2.5 feet below the ground surface. During the period of 110 days the electrical resistance changed from 18 Ω to 90 Ω, over 400% increase in the resistance.

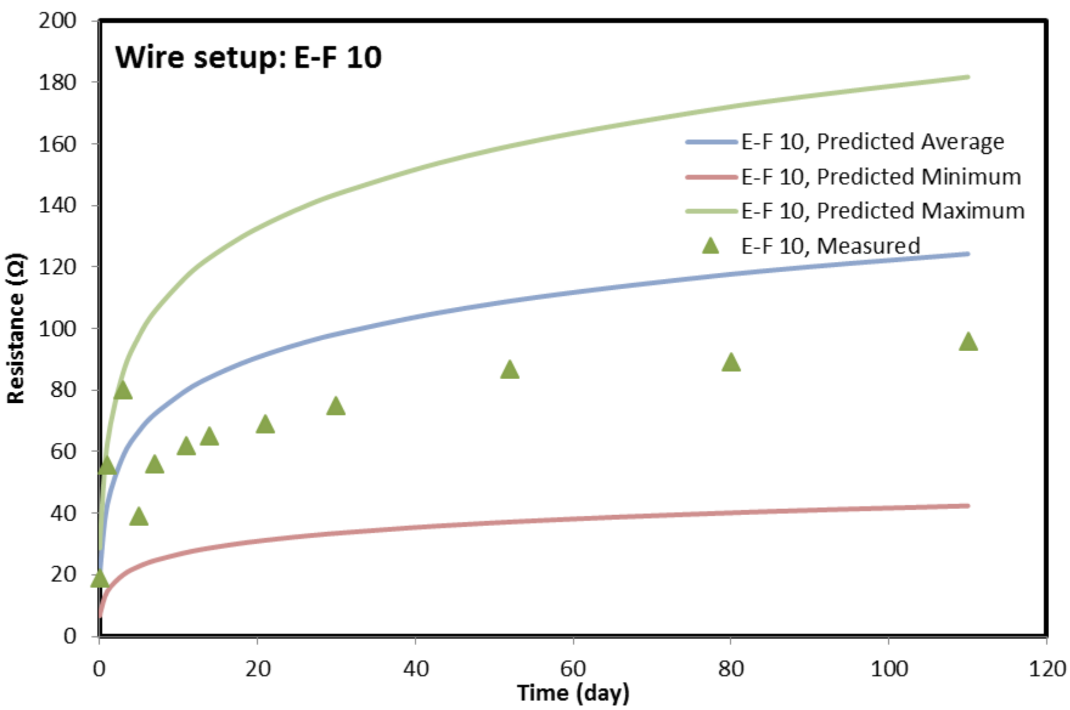

Figure 14. Comparing the Predicted and Measured Resistance for Horizontal Probes E10-F10.

Pressure Test

To simulate a pressure test, air pressure (Pi) was applied inside the tube (Fig. 15) to verify the piezoresistivity of the cement-sheath. Initially the electrical resistances (Ro in Ohms) was measured entire depth. These values were monitored while the air pressure was applied inside the casing (Figure 16) at a depth of 5 feet to a specific length of 18 inches using an expanding bladder. This test was done to demonstrate the sensitivity of the wmart cement to the applied small pressures.

Case 1: Pi = 10 psi: Internal pressure of 10 psi was applied and the resistance changes were measured immediately. The change in resistance was normalized with initial resistance ΔR/R(%) is shown in Fig.15. The resistivity change in the smart cement due to the applied pressure was about 0.8 to 1.6 percent, indicating the piezoresistivity of the smart cement.

Case 2: Pi = 20 psi: Pressure of 20 psi was applied and the resistance changes were measured immediately and reported in the form of ΔR/R (%) in Fig. 15. The resistivity change in the smart cement due to the applied pressure of 20 psi was about 1.0 to 2.3 percent and was varying with the depth, indicating the piezoresistivity of the smart cement.

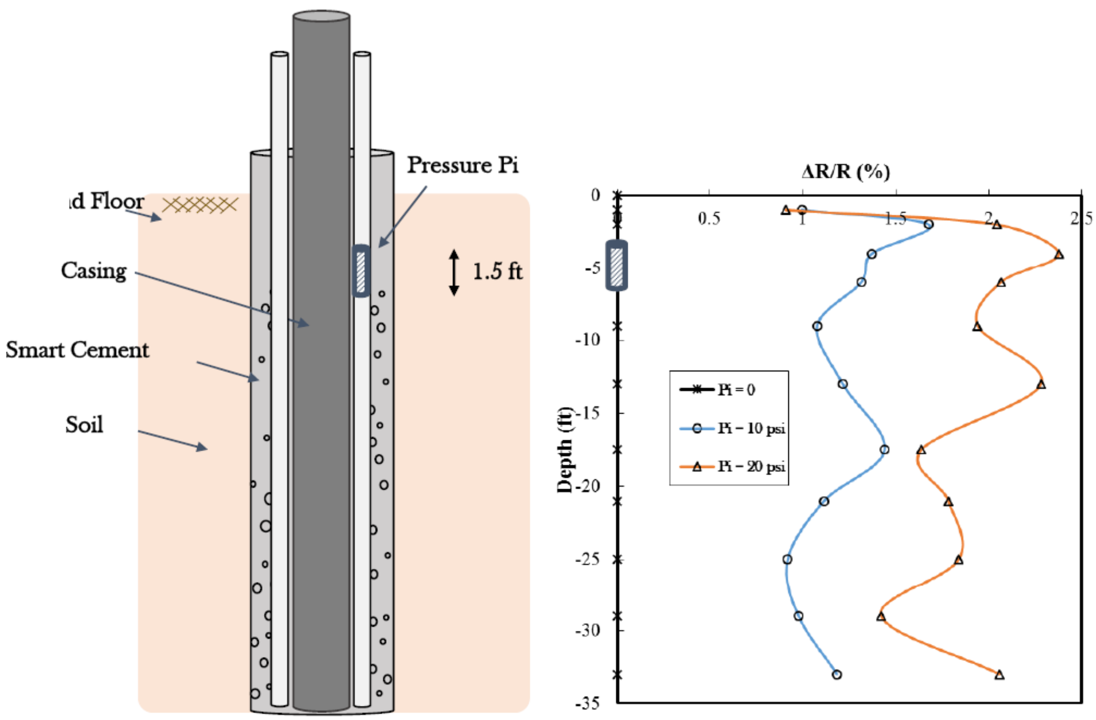

Figure 15. Variation of Initial Resistance with Depth after 100 Days of Curing

Piezoresistive modeling: The stress at every point can be separated into mean stress and deviatoric stress. The change in the deviatoric stress due to an applied pressure (Pi) along the axis of the casing (z-axis) is represented as ΔS_{zz}. Using equilibrium and stress analyses, it can be shown that ΔS_{zz} is directly proportional to the applied internal pressure, Pi (Eqn. 5). Hence, the change in deviatoric stress can be represented as follows:

$$\Delta S_{zz} = f(Pi) \tag{7}$$

The variation of internal applied pressure with the resistivity of smart cement ($\Delta\rho_Z/\rho_Z$ is shown in Fig. 16, and the response of the smart cement is shown to be nonlinear.

p-q model (Vipulanandan et al. (1990))

The nonlinear p-q model was developed by Vipulanandan et al. (1990) and was used to predict $\Delta\rho_Z/\rho_Z$ variation with the applied pressure. The relationship can be represented as follows:

$$p_i(\frac{\Delta\rho}{\rho}) = \frac{\left(\frac{\Delta\rho}{\rho}\right)}{q + (1-p-q)\left(\frac{\Delta\rho}{\rho}\right) + p\left(\frac{\Delta\rho}{\rho}\right)^{\frac{p}{q-p}}} \tag{8}$$

The model parameters p and q were 0.89 and 0.28, respectively. Hence, it is possible to predict the pressure in the casing using Eqn. (8) and also the stress in the cement sheath using Eqn. (5) by measuring the change in resistivity of the smart cement.

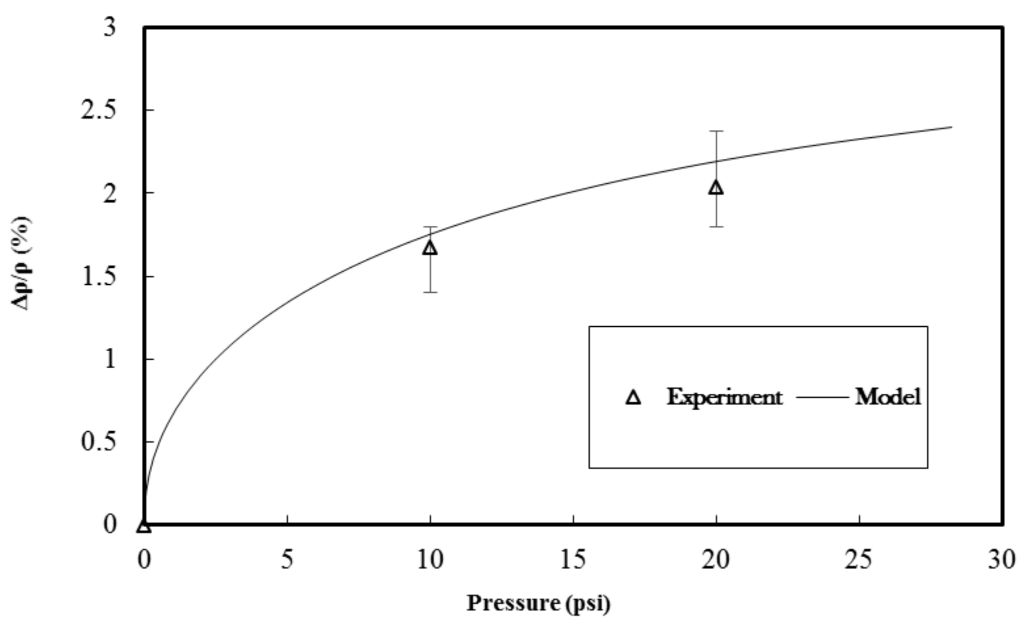

Figure 16. Model Predictions of Changes in Resistivity with Applied Pressure for Smart Cement after 100 Days of Curing

Conclusions

Based on the resistivity monitoring of the field test following conclusions are advanced.

(1) The two-probe method was effective in measuring the bulk resistance of the drilling fluid, and smart cement slurries. Based on the changes in resistance measurements it will be possible to identify the fluid rise in the well borehole.

(2) Field test demonstrate the real-time monitoring of the well bore with drilling fluid and smart cement slurries. During the installation of the field well

(3) Based on the concept developed in this study, it was possible to use the K parameter to predict the changes in the resistance of the hardening of smart cement. The predictions agreed well with the experimental results.

(4) The smart cement used to cement the field well was very sensitive to the applied pressure, piezoresistive cement. Using a nonlinear p-q model the change in electrical resistivity of smart cement was related to the applied pressure in the casing.

(5) Models have been developed to represent the curing of the cement under various conditions. It is possible to predict the pressure in the casing using Eqn. (8) and also the stress in the cement sheath using Eqn. (5) by measuring the change in resistivity of the smart cement.

Acknowledgements

This study was supported by the Center for Innovative Grouting Materials and Technology (CIGMAT) and the Texas Hurricane Center for Innovative Technology (THC-IT) at the University of Houston, Texas. Funding for the project (Project No. 10121-4501-01) is provided through the "Ultra-Deepwater and Unconventional Natural Gas and Other Petroleum Resources Research and Development Program" authorized by the Energy Policy Act of 2005. This program—funded from lease bonuses and royalties paid by industry to produce oil and gas on federal lands—is designed to assess and mitigate risk enhancing the environmental sustainability of oil and gas exploration and production activities. RPSEA is under contract with the U.S. Department of Energy's National Energy Technology Laboratory to administer three areas of research. RPSEA is a 501(c)(3) nonprofit consortium with more than 180 members, including 24 of the nation's premier research universities, five national laboratories, other major research institutions, large and small energy producers and energy consumers. The mission of RPSEA, headquartered in Sugar Land, Texas, is to provide a stewardship role in ensuring the focused research, development and deployment of safe and environmentally responsible technology that can effectively deliver hydrocarbons from domestic resources to the citizens of the United States. Additional information can be found at www.rpsea.org.

References

1. API Recommended Practice 10B (1997), Recommended Practice for Testing Well Cements Exploration and Production Department, 22nd Edition.

2. API Recommended Practice 65 (2002), Cementing Shallow Water Flow Zones in Deepwater Wells.

3. Carter, K. M. and Oort, E. (2014), Improved Regulatory Oversight Using Real- Time Data Monitoring Technologies in the Wake of Macondo, SPE 170323, pp. 1-51.

4. Izon, D. and M. Mayes, M. (2007), "Absence of fatalities in blowouts encouraging in MMS study of OCS incidents 1992-2006," Well Control Magazine, pp. 86-90.

5. John B., (1992). "Class G and H Basic Oil Well Cements," World Cement.

6. Kyle, M. and Van Eric (2014), Improved regulatory oversight using real- time data monitoring technologies in the Wake of Macondo, SPE 170323, pp. 1-51.

7. Vipulanandan, C. and Paul, E. (1990) "Performance of epoxy and polyester polymer concrete," ACI Materials Journal, Vol. 87, No. 3, pp. 241–251.

8. Vipulanandan, C., and Sett, K. (2004), "Development and Characterization of Piezoresistive Smart Structural Materials", Proceedings, Engineering, Construction and Operations in Challenging Environments, Earth & Space 2004, ASCE Aerospace Division, League City, TX, pp. 656-663.

9. Vipulanandan, C., and Liu, J. (2005), "Polyurethane Based Grouts for Deep Off-Shore Pipe-in-Pipe Application", Proceedings, Pipelines 2005, ASCE, Houston, TX, pp. 216-227.

10. Vipulanandan, C., and Garas, V. (2006), "Piezoresistivity of Carbon Fiber Reinforced Cement Mortar", Proceedings, Engineering, Construction and Operations in Challenging Environments, Earth & Space 2006, Proceedings ASCE Aerospace Division, League City, TX, CD-ROM.

11. Vipulanandan, C., Dimrican, E., and Harendra, S. (2010), "Artificial Neural Network and Nonlinear Models for Gelling and Maximum Curing Temperature Rise in Polymer Grouts," Journal of Materials in Civil Engineering, Volume 23, No. 4, p. 1-6.

12. Vipulanandan, C. and Prasanth, P., (2013)" Impedance Spectroscopy Characterization of a piezoresistive Structural Polymer Composite Bulk Sensor," Journal of Testing and Evaluation, Vol. 41, No.6, 898-904.

13. Vipulanandan et al. (2014a), "Development and Characterization of Smart Cement

for Real Time Monitoring of Ultra-Deepwater Oil Well Cementing Applications, OTC-25099-MS.

14. Vipulanandan et al. (2014b), "Characterization of Smart Cement Modified with Sodium Meta Silicate for Ultra-Deepwater Oil Well Cementing Applications, AADE-2014.

15. Vipulanandan, C. Heidari, M., Qu, Q., Farzam, H., and Pappas, J. M. (2014c), "Behaviour of piezoresistive smart cement contaminated with oil based drilling mud," Offshore Technology Conference, OTC 25200-MS, pp. 1-14.

16. Vipulanandan, C. and Mohammed, A. (2014d), "Hyperbolic rheological model with shear stress limit for acrylamide polymer modified bentonite drilling muds," Journal of Petroleum Science and Engineering, 122 (2014), 38–47.

17. Vipulanandan, C., and Mohammed, A., (2015a) "Smart cement rheological and piezoresistive behavior for oil well applications." Journal of Petroleum Science and Engineering, V-135, 2015, pp. 50-58.

18. Vipulanandan, C., and Mohammed, A., (2015b) "Smart cement modified with iron oxide nanoparticles to enhance the piezoresistive behavior and compressive strength for oil well applications." Journal of Smart Materials and Structures, Vol. 24 Number 12, pp. 1-11.

19. Vipulanandan, C, Krishnamoorti, R. Mohammed, A., G. Narvaez, Head, B. and Pappas, J. (2015c) "Iron Nanoparticle Modified Smart Cement for Real Time Monitoring of Ultra Deepwater Oil Well Cementing Applications", Offshore Technology Conference (OTC) 2015, OTC-25842-MS, pp. 1-20.

20. Vipulanandan, C, Ramanathan, P. Ali, M., Basirat, B. and Pappas, J. (2015d) "Real Time Monitoring of Oil Based Mud, Spacer Fluid and Piezoresistive Smart Cement to Verify the Oil Well Drilling and Cementing Operation Using Model Tests", Offshore Technology Conference (OTC) 2015, OTC-25851-MS, pp. 1-18.

21. Zhang, M., Sisomphon, K., Ng, T.S, and Sun, D.J, (2010a). "Effect of superplasticizers on workability retention and initial setting time of cement pastes," Construction and Building Materials 24, 1700–1707.

22. Zhang, J., Weissinger, E.A, Peethamparan, S, and Scherer, G.W., (2010b). "Early hydration and setting of oil well cement," Cement and Concrete research, Vol. 40, 1023-1033.